ESC European Society of Cardiology

European Heart Journal - Cardiovascular Imaging (2020) **0**, 1–8
doi:10.1093/ehjci/jeaa212

Multimodality cardiac evaluation in children and young adults with multisystem inflammation associated with COVID-19

Paraskevi Theocharis[1]*†, James Wong [1]†, Kuberan Pushparajah[1,2], Sujeev K. Mathur[1], John M. Simpson[1], Emma Pascall[1], Aoife Cleary[1], Kirsty Stewart[1], Kaitav Adhvaryu[1], Alex Savis[1], Saleha R. Kabir[1], Mirasol Pernia Uy[1], Hannah Heard[1], Kelly Peacock[1], and Owen Miller[1,3]

[1]Department of Paediatric Cardiology, Evelina London Children's Hospital, UK; [2]School of Biomedical Engineering and Imaging Sciences, King's College London, UK; and [3]Department of Women and Children's Health, Faculty of Life Science and Medicine, King's College London, UK

Received 1 July 2020; editorial decision 2 June 2020; accepted 4 July 2020

Aims Following the peak of the UK COVID-19 epidemic, a new multisystem inflammatory condition with significant cardiovascular effects emerged in young people. We utilized multimodality imaging to provide a detailed sequential description of the cardiac involvement.

Methods and Results Twenty consecutive patients (mean age 10.6 ± 3.8 years) presenting to our institution underwent serial echocardiographic evaluation on admission (median day 5 of illness), the day coinciding with worst cardiac function (median day 7), and the day of discharge (median day 15). We performed cardiac computed tomography (CT) to assess coronary anatomy (median day 15) and cardiac magnetic resonance imaging (CMR) to assess dysfunction (median day 20). On admission, almost all patients displayed abnormal strain and tissue Doppler indices. Three-dimensional (3D) echocardiographic ejection fraction (EF) was <55% in half of the patients. Valvular regurgitation (75%) and small pericardial effusions (10%) were detected. Serial echocardiography demonstrated that the mean 3D EF deteriorated (54.7 ± 8.3% vs. 46.4 ± 8.6%, $P = 0.017$) before improving at discharge ($P = 0.008$). Left main coronary artery (LMCA) dimensions were significantly larger at discharge than at admission (Z score –0.11 ± 0.87 vs. 0.78 ± 1.23, $P = 0.007$). CT showed uniform coronary artery dilatation commonly affecting the LMCA (9/12). CMR detected abnormal strain in all patients with global dysfunction (EF <55%) in 35%, myocardial oedema in 50%, and subendocardial infarct in 5% (1/20) patients.

Conclusions Pancarditis with cardiac dysfunction is common and associated with myocardial oedema. Patients require close monitoring due to coronary artery dilatation and the risk of thrombotic myocardial infarction.

Keywords Hyper-inflammatory syndrome • Kawasaki • PIMS-TS • MIS-C • COVID-19 • SARS-CoV-2

Introduction

During the COVID-19 pandemic, our group[1,2] and others in Europe[3–5] and the USA[6] have described cohorts of children and young adults presenting as a hyperinflammatory syndrome with multiorgan involvement, with features similar to Kawasaki disease shock syndrome (KDSS), toxic shock syndrome (TSS), haemophagocytic lymphohistiocytosis (HLH), and macrophage activation syndrome (MAS) induced by a cytokine storm.[1,3] This new condition has arisen after the peak of the SARS-CoV-2 pandemic in the respective countries. The novel syndrome has been named paediatric inflammatory multisystem syndrome temporally associated with SARS-CoV-2

* Corresponding author. Department of Paediatric Cardiology, Evelina London Children's Hospital, London SE1 7EH, UK. Tel: +44 20 7188 7188, Email: paraskevi.theocharis@gstt.nhs.uk
† These authors contributed equally to this work.

infection (PIMS-TS) in a case definition published by the Royal College of Paediatrics and Child Health (RCPCH)[7] or multisystem inflammatory syndrome in children (MIS-C).[8] Very similar case definitions have been published in the UK, in the USA, and by the World Health Organization.[9]

Cardiac involvement has been reported in those with PIMS-TS.[1–6] However, a detailed description of cardiac manifestations of this syndrome is lacking. We present the comprehensive results of sequential multimodality cardiac imaging with echocardiography, computed tomography (CT), and cardiac magnetic resonance imaging (CMR) in the first 20 unselected sequential patients with this syndrome at our centre.

Methods

This was a retrospective single institution study of the cardiac imaging manifestations in consecutive patients presenting to the Evelina London Children's Hospital (ELCH) with features of PIMS-TS as defined by the RCPCH, UK.[7] Imaging was performed with local ethical approval (08/H0810/058).

Clinical and laboratory evaluation

Demographic data and SARS-CoV-2 case contacts were collected from hospital notes. Vital signs and cardiac biomarkers including troponin-T and N-terminal probrain natriuretic peptide (NT-proBNP) were collected prospectively.

Cardiac imaging evaluation protocol

All patients had echocardiographic evaluation on admission. Echocardiograms were performed daily during the acute phase of the disease, and on alternate days during the recovery phase. We defined three time points for analysis: echocardiogram on admission; echocardiogram based on worst three-dimensional (3D) ejection fraction (EF) during the hospital admission; and discharge echocardiogram. As this is an emerging disease with evolving cardiac involvement of an unknown extent and course, we performed further cross-sectional cardiac imaging (CT and CMR) to determine: coronary artery dimensions; myocardial characterization; and functional parameters.

Echocardiography

Philips IE33 and EPIQ 7C echocardiography systems (Philips Medical Systems, Andover, MA, USA) were used to obtain imaging with offline processing using Philips IntelliSpace Cardiovascular (ISCV) and analysis using QLAB, Version 10.8.5 (Philips Medical Systems).

The echocardiogram included extensive functional assessment. Left ventricular (LV) function was quantified in accordance with published guidelines,[10] and *Z* scores were calculated where appropriate.[11]

Peak pulsed wave tissue Doppler imaging (TDI) systolic and diastolic velocities of the basal septal and lateral segments of the left ventricle were analysed according to published standards.[12] The LV diastolic function and LV filling pressures were assessed.[13,14] The four-chamber, three-chamber, and two-chamber views were used for 2D based speckle-tracking myocardial deformation echocardiographic analysis. 3D echocardiography was used to calculate LV volumes and EF.[15]

The dimensions of the coronary arteries were expressed as *Z* scores in accordance with the published reference standard.[16] Coronary artery dilation was defined by the presence of a *Z* score >2 in the affected segment.

All echocardiographic measurements and reports were reviewed prospectively by consultants with subspecialty expertise in echocardiography (PT, JW, KP, and OM).

Cardiac computed tomography

Prospectively ECG-gated coronary CT angiography was performed using a Somatom Force scanner (Siemens Healthcare AG, Erlangen, Germany). Scans were performed urgently in the presence of echocardiographic evidence of rapidly evolving coronary dilatation. Imaging was acquired at end-systole defined by the end of the T-wave. Intravenous contrast (Omnipaque^{TM} 350) was administered at 1.5–2.0 mL/kg and monitoring slices were used to determine maximal contrast density in the descending aorta. The mean dose–length product was low at 46.2 mGy·cm for cohort mean body surface area (BSA) of 1.4 m^2. Images were analysed using SECTRA-PACS (Sectra AB, Linkoping Sweden). Intraluminal diameters of the coronary artery segments were measured in two dimensions using multiplanar reconstruction (MPR) by two blinded observers (J.W. and S.M.). The mean value was recorded, and *Z* scores were calculated as per Dallaire *et al.*,[16] in keeping with the literature on extrapolating coronary CT measurements from echocardiographic datasets.[17]

Cardiac magnetic resonance

Retrospectively ECG-gated balanced steady-state free precession (bSSFP) cine imaging was acquired in short- and long-axis orientations of the heart including two-chamber, three-chamber, and four-chamber views. Field of view was optimized to cover the chest wall. Typical imaging parameters were: parallel imaging factor (SENSE) 2; in-plane resolution 2 × 2 mm; slice thickness 8 mm in the long axis and 8–10 mm in the short axis; and temporal resolution 30 phases. Myocardial inflammation was assessed in accordance with the Lake Louise CMR criteria.[18] Due to the lack of consistent reference normal values in native T1 mapping and T2 relaxation times in children, myocardial oedema was characterized by increased signal intensity on T2-weighted imaging and myocardial injury was characterized by the presence of non-ischaemic patterns of late gadolinium enhancement (LGE). Evidence of myocardial oedema with T2 hyperintensity was defined as:

$$\text{T2 ratio} > 2$$

where: T2 ratio = $\text{signal}_{\text{intensity myocardium}}/\text{signal}_{\text{intensity skeletal muscle}}$.

A Look–Locker sequence was performed to assess inversion time 5 min after administration of 0.1 ml/kg i.v. gadobutrol (Gadovist, Bayer Schering Pharma, Germany). Phase-sensitive inversion recovery (PSIR) was used to assess for LGE. CMR 42 (Circle Cardiovascular Imaging, Canada) was used to measure LV volumes, feature tracking global strain indices (short axis for circumferential strain; mean long-axis values for longitudinal strain; radial strain was not assessed due to poor interuser variability), and assess for evidence of myocardial necrosis and fibrosis.

Statistical analysis

Statistical analysis was performed using SPSS v. 26. Interobserver variability of CMR LV volume segmentation and CT coronary artery measurements were quantified using an intraclass coefficient two-way model with absolute agreement. Measurements were sampled for 10 subjects by two authors (J.W. and K.P. for CMR data; J.W. and S.M. for CT data). Variables were tested for normality using the Kolmorgorov–Smirnov test. Repeated measures analysis of variance (RM ANOVA) was performed to evaluate changes of all echocardiographic parameters assessed on admission, during hospitalization, and at discharge. The results for variables with normal distribution were reported as mean ± SD, while the non-normally distributed parameters were reported as median (range). Statistical significance was defined as a two-tailed *P*-value of <0.05.

Table 1 Demographic data including day of presentation with illness, day of worst dysfunction, and timing of imaging

ID	Age (years)	Gender	Ethnicity	Day of presentation	Day of worst dysfunction	Day of discharge	Day CT performed	Day MRI performed
1	8	M	1	3	12	25	12	25
2	13	F	1	5	6	14	12	14
3	6	M	2	4	12	15	19	21
4	6	F	1	6	8	11	23	25
5	12	M	1	5	8	17	16	17
6	8	F	1	4	5	15	21	23
7	12	F	1	3	4	13	6	16
8	11	M	2	5	8	13	27	28
9	5	M	4	6	7	15	27	18
10	14	M	1	2	8	10	26	25
11	14	M	4	5	8	13	14	21
12	9	M	2	5	8	14	12	17
13	4	F	1	2	6	14	9	21
14	15	M	1	6	7	15	10	18
15	7	M	5	5	7	12	22	20
16	16	M	5	4	6	13	9	21
17	11	M	2	4	7	16	23	16
18	11	M	1	2	4	9	8	19
19	16	M	1	4	10	17	22	29
20	15	M	1	3	4	9	4	11
Median (range)	11 (4–16 years)	15M:5F	1 (n = 12), 2 (n = 4), (n = 0), 4 (n = 2), 5 (n = 2)	5 (2–6 days)	7 (4–12 days)	15 (11–25 days)	15 (4–27 days)	20 (11–29 days)

Ethnicity key: 1, Black/African/Caribbean/Black British; 2, Asian/Asian British; 3, mixed/multiple ethnic groups, 4, White (UK); 5, White (other).

Ethics

This study complies with the Declaration of Helsinki. Local ethical approval was received (08/H0810/058).

Results

Demographics

The first 20 patients fulfilling diagnostic criteria for PIMS-TS treated during a 22-day period (16 April–8 May 2020) were included. Demographics are outlined in *Table 1*. Median duration of symptoms at time of presentation was 5 days (range 2–7 days). Mean age was 10.6 ± 3.8 years (range 4–16 years). Fifteen (75%) patients were male and 19 (95%) tested positive for either IgM or IgG antibodies to COVID-19. Two of the 19 antibody-positive patients had positive SARS-CoV-2 PCR from oropharyngeal swab sampling. Worst cardiac function, as determined by 3D echo EF, occurred on a median of 7 days (range 4–12 days) after the onset of the illness. Median patient discharge occurred after 15 days (range 11–25 days) of the illness and clinically corresponded to defervescence and normalization of inflammatory markers.

Admission echocardiography findings

On admission, five patients (25%) demonstrated subjectively increased echogenicity of the interventricular septum when compared with the rest of the myocardium, while all had increased pericardial brightness (*Figure 1*; Supplementary material online, *Video 1*). Eight patients (40%) presented with impaired LV systolic performance [M-mode-derived LV fractional shortening (FS) <30%]. 3D echocardiography assessment revealed that 10 (50%) patients presented with reduced LV systolic function (3D LVEF <55%). However, LV systolic performance, assessed by TDI and strain echocardiography, was reduced in 18 (90%) patients. Mean 2D-derived global longitudinal strain (GLS) was –13.2 ± 2.9% (range –7.0% to –18.8%). TDI echocardiography showed that nine (45%) patients had an E/e' >8 in keeping with evidence of increased LV filling pressures; this did not correlate with serum NT-proBNP levels. On admission, 10 (50%) patients had mild mitral regurgitation (MR) and 12 (60%) had mild tricuspid regurgitation (TR). Two patients presented with moderate to severe MR and three patients with moderate to severe TR. One patient had trivial aortic regurgitation (AR) and two were found to have pericardial effusion on admission. Echocardiographic coronary assessment revealed that three patients (15%) had already developed coronary artery dilatation.

Serial echocardiography assessment

All patients underwent serial echocardiographic assessments during their hospital stay. While LV systolic function, assessed by M-mode-derived FS, did not change during the hospitalization period compared with the admission echocardiography (P = 0.95 and P = 0.92, respectively), there was a subsequent significant improvement noted on the discharge echocardiogram (FS 29.6 ± 10.1% vs. 39.2 ± 7.0%,

P = 0.002). The observations regarding LV systolic performance were confirmed by TDI echocardiography and 2D-derived GLS. In keeping with FS remaining unchanged between admission and during hospitalization, the recorded septal and lateral TDI velocity Z scores (s'_{sep} and s'_{lat}) also did not differ significantly (P = 0.34 and P = 0.60, respectively). Similarly the GLS recorded on admission did not change significantly (P = 0.40) during hospitalization. Overall there was significant improvement of the systolic septal and lateral TDI velocities and the 2D-derived GLS from admission to discharge (s'_{sep} TDI 6.9 ± 1.4 cm/s vs. 8.1±1.6 cm/s, P = 0.014; s'_{lat} TDI 8.0 ± 1.6 cm/s vs. 9.4 ± 2.1 cm/s, P = 0.007; and GLS –11.9 ± 7.6% vs. –17.0 ± 2.9%, P = 0.018). 3D echocardiography appeared to be more sensitive to identify a significant change from baseline assessment during the admission period (54.7 ± 8.3% vs. 46.4 ± 8.6%, P = 0.017) and a subsequent significant improvement on discharge (46.4 ± 8.6% vs. 68.6 ± 7.5%, P = 0.008). LV diastolic function, assessed by E/A and E/e' ratios, did not significantly change during serial echocardiographic assessments. However, TDI echocardiography demonstrated that the late diastolic velocities of the lateral aspect of the mitral annulus (a'_{lat}) during admission were significantly reduced, which was a sustained finding throughout hospitalization (*Table 2*).

On admission echocardiography, two patients (10%) had left anterior descending (LAD) dilatation (Z score >2) and one patient (5%) had right coronary artery (RCA) dilatation. Eight patients developed coronary dilatation during the hospital admission (*Figure 2*; Supplementary material online, *Video 2*). On discharge, coronary

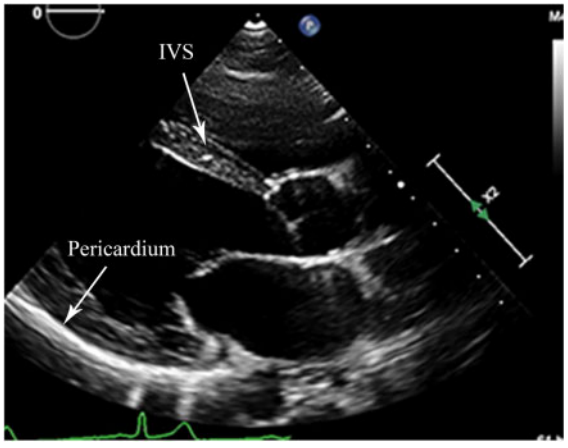

Figure 1 Long-axis parasternal view of the left ventricle from the same patient as shown in Supplementary material online, *Video 1*, demonstrating the increased echogenicity of the interventricular septum (collection of bright spots) and very bright pericardium.

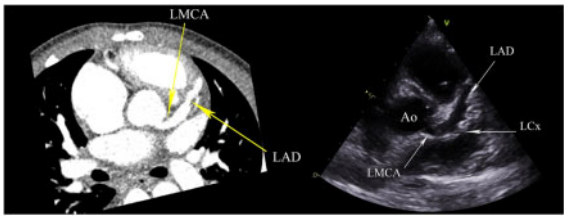

Figure 2 Short-axis view of the heart at the level of the aortic valve on CT and echocardiogram showing diffuse ectatic changes in the left main coronary artery (LMCA) and left anterior descending (LAD) artery. The circumflex artery origin can just be seen coming off the LMCA and is ectatic in configuration.

Table 2 Serial echocardiographic measurements

	Admission echo (1)	In-hospital echo (2)	*P* (echo 1 vs. echo 2)	Echo at discharge (3)	*P* (echo 2 vs. echo 3)
FS (M-mode), %	30.2 ± 9.1	29.6 ± 10.1	0.928	39.2 ± 7.0	0.002
3D LVEF, %	54.7± 8.3	46.4± 8.6	0.017	68.6 ± 7.5	0.008
GLS	–13.2 ± 2.9	–11.9 ± 7.6	0.406	–17.0 ± 2.9	0.018
MV E/A	1.77 ± 0.30	2.08 ± 0.98	0.377	1.76 ± 0.40	0.419
E/e'	8.3 ± 2.1	8.5 ± 3.4	0.807	7.1 ± 1.0	0.120
s'_{sep}, cm/s	7.4 ± 1.6	6.9 ± 1.4	0.366	8.1 ± 1.6	0.014
s'_{sep}, Z score	–0.56 ± 1.25	–0.90 ± 0.99	0.340	–0.03 ± 1.20	0.014
s'_{lat}, cm/s	8.7 ± 2.5	8.0 ± 1.6	0.502	9.4 ± 2.1	0.007
s'_{lat}, Z score	–0.74 ± 0.95	–0.87 ± 0.59	0.603	–0.35 ± 0.68	0.021
e'_{lat}, Z score	–1.45 ± 1.46	–1.77 ± 1.14	0.211	–1.76 ± 1.08	0.976
a'_{lat}, Z score	1.31 ± 2.98	–0.31 ± 2.98	0.013	–0.50 ± 1.06	0.803
TAPSE, mm	19.0 ± 4.5	18.6 ± 4.4	0.772	23.0 ± 2.3	0.009
LMCA, Z score	–0.11 ± 0.87	0.23 ± 1.37	0.242	0.78 ± 1.23	0.108
LAD, Z score	0.65 ± 1.22	1.16 ± 2.42	0.409	1.58 ± 2.71	0.183
LCx, Z score	–1.15 ± 0.79	–0.69 ± 1.32	0.149	–0.88 ± 1.07	0.597
RCA, Z score	–0.11 ± 1.24	0.51 ± 1.41	0.026	0.16 ± 1.53	0.062

FS, fractional shortening; LVEF, left ventricular ejection fraction; GLS, global longitudinal strain; MV, mitral valve; TAPSE, tricuspid annular plane systolic excursion; LMCA, left main coronary artery; LAD; left anterior descending; LCx, left circumflex; RCA, right coronary artery.

Table 3 CT-derived coronary artery measurements

ID	*Z* score			
	Right coronary artery	Left main coronary artery	Left anterior descending	Left circumflex
1	5.0	5.5	12.2	3.0
2	0.6	3.2	3.5	–
3	0.7	0.5	1.6	0.7
4	–1.1	0.5	0.3	0.6
5	–1.0	1.2	1.5	0.8
6	–1.2	2.0	1.6	–0.1
7	0.2	3.5	3.5	1.7
8	0.5	–0.1	0.1	-0.9
9	2.0	0.9	1.8	-1.8
10	–1.9	–0.8	0.1	0.2
11	–0.6	2.3	2.6	0.3
12	0.3	–0.2	1.4	0.2
13	1.0	3.8	4.1	2.2
14	0.8	1.0	3.0	0.3
15	-0.7	1.4	1.8	0.6
16	0.9	2.1	3.2	0.9
17	–1.1	2.4	2.0	–0.4
18	0.1	1.7	2.4	0.1
19	–0.9	0.6	0.9	–1.9
20	0.9	1.7	4.3	0.5

Z score values are extrapolated from echocardiography.

artery dilatation was seen in the left main coronary artery (LMCA) in two patients (10%), in the LAD in four patients (20%), and in the RCA in two patients (10%). No patients had persistent left circumflex (LCx) dilatation. Echocardiographic assessment of the coronary arteries revealed gradual serial dilatation of the LMCA from initial presentation, reaching statistical significance on *Z* score values (0.78 ± 1.23 vs. –0.11 ± 0.87, $P = 0.007$). There were no observed serial significant changes to the size of the LAD and the LCx. While the RCA initially demonstrated a change in size (*Z* scores –0.11 ± 1.24 vs. 0.51 ± 1.41, $P = 0.026$), its size subsequently demonstrated considerable recovery (0.51 ± 1.4 vs. 0.16 ± 1.53, $P = 0.062$) (see *Table 2*).

Cardiac computed tomography

All patients underwent cardiac CT imaging, at a median time of 15 days (range 4–27 days) after the onset of their illness with adequate coronary imaging in all studies (*Table 3*). Twelve patients (60%) showed coronary artery ectasia (*Z* score >2) with no segmental aneurysms. The distal coronary arteries were not involved. The left coronary artery system was affected in all 12 patients, with additional involvement of the RCA in two patients. One patient had involvement of the LMCA, LAD, LCx, and the RCA. Both the LMCA and LAD were dilated in 9/12 patients, and the LAD in isolation in 3/12 patients. When LMCA dilatation occurred, the origin of the LMCA was also involved. The *Z* scores for the coronary arteries for all but one patient corresponded to small aneurysms (*Z* score <5) as defined by Friedman *et al.*[19] The pattern of uniform dilatation including the origin and continuous varying lengths of the proximal vessels (with no segmental distribution) appeared to lend itself to a description of ectasia rather than aneurysm[20] (*Table 3*). One patient had congenital absence of the LCx.

The intraclass coefficient (95th confidence interval) for measurement of all coronary arteries was 0.951 (0.925–0.971), $P < 0.0001$.

Cardiac magnetic resonance

All patients underwent CMR, with seven of these under general anaesthetic (*Table 4*). Median time to MRI was 20 days (range 11–29 days) after the onset of illness. Mean indexed left ventricular end-diastolic volume (iLVEDV), indexed left ventricular end-systolic volume (iLVESV), and indexed left ventricular stroke volume (iLVSV) were within normal range corrected for BSA. Global function measured by LVEF demonstrated 13 patients with normal function (EF >55%), 3 patients with borderline dysfunction (EF 50–55%), and 4 patients with mild LV dysfunction (EF <50%). There was mild right ventricular (RV) dysfunction in one patient.

Myocardial oedema was present in 10 patients (50%). Global increase in T2-weighted imaging was most commonly observed ($n = 6$) followed by the basal septal segments ($n = 3$). Strikingly, global MR strain analysis demonstrated that every patient had impairment in systolic strain indices in at least one axis compared with normal values.[21] Those with the worst function (EF and strain) did not correlate with persistent myocardial oedema, scarring, age, or timing of presentation. Intraclass coefficient (95th confidence interval) was 0.97 (0.80–0.99) for EDV, 0.95 (0.80–0.98) for ESV, 0.95 (0.82–0.98) for SV, and 0.89 (0.58–0.97) for EF.

Adverse findings

One patient developed acute heavy central chest pain during admission with evolving ECG changes and a sharp rise in cardiac enzymes. Echocardiography demonstrated no change in LV function. Cardiac CT showed a dilated LAD and LCx with no obvious thrombus. CMR assessment found LGE in the infero-lateral basal wall of the endocardium and myocardium consistent with a subendocardial myocardial infarction in the territory supplied by the dilated coronary system (*Figure 3*).

Discussion

This novel multisystem inflammatory syndrome has been differentiated from KD and KDSS and is thought to be a new disease entity temporally associated with prior exposure to SARS-CoV-2 infection.[2] A striking feature is the high degree of cardiovascular compromise, often with circulatory shock, myocardial depression, and coronary involvement. Using multimodality analysis, we show that the extent of cardiac involvement is greater than first reported,[3–5] with LV dysfunction, myocardial oedema, and coronary artery changes persisting even after clinical defervescence and normalization of inflammatory markers.

While coronary involvement in KD occurs in 23–50% of cases,[22,23] in this cohort of patients we found a higher incidence (60%) of cases with enlarged coronary arteries and a distinctive pattern of involvement: (i) the LCx and RCA were never affected in isolation; (ii) the orifice of the LMCA was frequently ectatic; and (iii) dilatation of the

Table 4 Cardiac magnetic resonance imaging data showing volumetric, functional, and late gadolinium enhancement pattern

ID	iLVEDV (mL/m^2)	iLVESV (mL/m^2)	iLVSV (mL/m^2)	LVEF (%)	iWall mass (g/m^2)	T2-weighted signal	LGE pattern	Pericardial effusion	Peak circumferential strain (%)	Peak longitudinal strain (%)
1	97	52	45	47	57	–	–	–	–15.0	–13.5
2	72	31	41	57	46	Septum	–	–	–16.7	–15.9
3	91	37	54	60	48	Septum	–	–	–16.7	–16.5
4	64	27	37	58	35	–	–	Small	–16.7	–11.9
5	101	45	56	56	52	Lateral wall	–	–	–16.1	–13.6
6	58	28	30	52	34	–	–	–	–17.6	–12.5
7	48	17	31	65	52	Global	Speckling	–	–19.1	–13.9
8	61	34	27	45	46	Global	Speckling	–	–18.3	–14.0
9	93	43	52	55	45	–	–	Small	–18.5	–11.5
10	78	38	40	51	52	–	–	–	–16.7	–13.7
11	97	47	51	52	65	–	–	–	–18.3	–17.1
12	75	18	56	76	35	–	–	–	–22.4	–18.5
13	79	32	47	59	53	–	–	Small	–18.8	–16.1
14	71	36	35	49	48	–	–	Small	–18.3	–16.0
15	81	32	49	60	64	Global	–	–	–18.5	–18.5
16	100	34	67	66	53	Global	–	–	–19.0	–16.2
17	71	16	55	78	36	Septum	–	Small	–19.8	–19.5
18	69	29	40	58	47	Global	–	–	–20.8	–17.0
19	83	42	40	48	43	Global	Speckling	–	–15.1	–11.1
20	94	33	61	64	69	–	Infarct	–	–19.8	–17.2
Mean	79.1	33.5	45.7	57.8	49.1				–18.1	–15.2
SD	15.3	9.6	10.9	8.9	9.9				1.8	2.5

iLVEDV, indexed left ventricular end-diastolic volume; iLVESV, indexed left ventricular end-systolic volume; iLVSV, indexed left ventricular stroke volume; LVEF, left ventricular ejection fraction, LGE, late gadolinium enhancement.

vessel was always uniformly ectatic. This is in contrast to KD where involvement is diffuse, the LMCA orifice is typically spared,[24] and there are often normal interposing segments between aneurysms.[20] The observed coronary changes in this new condition may be a prominent response to fever[25] and an underlying cytokine storm—reflected in the elevated inflammatory markers occurring with PIMS-TS[1]—rather than changes within the arterial wall that occur in KD.[25,26] It might be postulated that with resolution of inflammation there should be recovery of any findings temporally related to the inflammation.[27]

The incidence of coronary involvement was higher on CT compared with echocardiography, a consistent finding from other studies where 56% of aneurysms may be missed by echocardiography alone.[17] Existing data suggest that CT is an excellent tool for assessing coronary aneurysms in KD,[28] with good correlation to established echocardiographic parameters and permitting better detection particularly of smaller lesions which have been noted in this patient group.[29]

There was echocardiographic evidence of cardiac involvement affecting LV systolic and diastolic performance in all patients studied, which is greater than with previous studies.[2,3,5] In a study of a similar inflammatory syndrome, 60% had some form of cardiac involvement; however, only 2D EF or the presence of coronary abnormalities was recorded.[3] In our study, a significant proportion of patients had abnormal LV systolic function on admission, and serial echocardiograms demonstrated that LV dysfunction evolved, typically worsening by day 7 of the illness on a range of echocardiographic modalities. Even though LV dysfunction, by means of M-mode FS, was identified in a significant proportion of patients, this is likely to be an underestimate of the true extent of the overall LV systolic dysfunction.[5] The use of 3D echocardiography revealed that a higher proportion of the patients had affected LV systolic function on admission, which significantly worsened during hospitalization in line with deterioration of their clinical status. Similarly, at discharge, the 3D-derived LVEF normalized in almost all patients in keeping with their clinical improvement. The above findings were confirmed by the low GLS and the altered systolic TDI velocities in a significant proportion on admission, indicating that 3D LVEF may be a more sensitive marker for dysfunction in this group. In general, serial detailed echocardiographic assessment determined that functional cardiac involvement was more extensive than first thought. The process was not static and involved a pancarditis affecting the valves, the myocardium and causing pericardial effusions (25% on CMR). KD rarely causes such a frequency of cardiac impairment,[30] with valvular dysfunction occurring in 25% and ventricular dysfunction occurring in only 20%.[30]

LV dysfunction persisted in 35% of patients assessed by CMR-derived EF. However, we identified further subtle signs of ongoing dysfunction with abnormal strain patterns in all patients persisting beyond 2 weeks of the onset of the illness. Positive T1 and T2 criteria were present in 10 patients, suggesting that the extent of active

Figure 3 MRI: short axis view of the left ventricle showing late gadolinium enhancement imaging (indicated by arrow) of a transmural myocardial infarction.

myocardial inflammation was prominent but resolving and in keeping with the rapid clinical and echocardiographic recovery seen in patients following resolution of inflammation. It would be worth mentioning that one patient presented with a typical acute coronary syndrome caused by a subendocardial infarction. This demonstrates the need for high vigilance in this group of patients.

In conclusion, the major findings are that the extent of cardiac involvement is greater than first reported, with evolving cardiac impairment and coronary changes. Ongoing dysfunction, oedema, and coronary artery changes can persist despite defervescence and normalization of inflammatory markers. We propose that all patients who present with this novel multisystem inflammatory syndrome should be screened with basic, and then advanced, echocardiography supplemented by structured multimodality imaging.

Limitations and further work

This is a newly described condition and the data presented are retrospectively reviewed. We propose further collaborative work between institutions to streamline treatment pathways. A large number of patients had ongoing dysfunction and enlarged coronary arteries indicating the need for ongoing assessment and review of medium- to long-term outcomes.

Supplementary material

Supplementary material is available at *European Heart Journal – Cardiovascular Imaging* online.

Acknowledgements

We thank our colleagues across all specialties working as part of the Evelina PIMS-TS Working Group who worked tirelessly during the pandemic to deliver care for this challenging group of children.

Funding

O.M. has taught on foetal cardiology and cardiac imaging courses organized by Canon Medical and Philips Medical.

Conflict of interest: none declared.

References

1. Whittaker E, Bamford A, Kenny J, Kaforou M, Jones CE, Shah P, Ramnarayan P, Fraisse A, Miller O, Davies P, Kucera F, Brierley J, McDougall M, Carter M, Tremoulet A, Shimizu C, Herberg J, Burns JC, Lyall H, Levin M; PIMS-TS Study Group and EUCLIDS and PERFORM Consortia. Clinical characteristics of 58 children with a pediatric inflammatory multisystem syndrome temporally associated with SARS-CoV-2. *JAMA* 2020;doi: 10.1001/jama.2020.10369.
2. Riphagen S, Gomez X, Gonzalez-Martinez C, Wilkinson N, Theocharis P. Hyperinflammatory shock in children during COVID-19 pandemic. *Lancet* 2020; **395**:1607–1608.
3. Verdoni L, Mazza A, Gervasoni A, Martelli L, Ruggeri M, Ciuffreda M, Bonanomi E, D'Antiga L. An outbreak of severe Kawasaki-like disease at the Italian epicentre of the SARS-CoV-2 epidemic: an observational cohort study. *Lancet* 2020; **395**:1771–1778.
4. Belhadjer Z, Meot M, Bajolle F, Khraiche D, Legendre A, Abakka S, Auriau J, Grimaud M, Oualha M, Beghetti M, Wacker J, Ovaert C, Hascoet S, Selegny M, Malekzadeh-Milani S, Maltret A, Bosser G, Giroux N, Bonnemains L, Bordet J, Di Filippo S, Mauran P, Falcon-Eicher S, Thambo JB, Lefort B, Moceri P, Houyel L, Renolleau S, Bonnet D. Acute heart failure in multisystem inflammatory syndrome in children (MIS-C) in the context of global SARS-CoV-2 pandemic. *Circulation* 2020;doi: 10.1161/CIRCULATIONAHA.120.048360.
5. Ramcharan T, Nolan O, Lai CY, Prabhu N, Krishnamurthy R, Richter AG, Jyothish D, Kanthimathinathan HK, Welch SB, Hackett S, Al-Abadi E, Scholefield BR, Chikermane A. Paediatric inflammatory multisystem syndrome: temporally associated with SARS-CoV-2 (PIMS-TS): cardiac features, management and short-term outcomes at a UK tertiary paediatric hospital. *Pediatr Cardiol* 2020; doi: 10.1007/s00246-020-02391-2.
6. Cheung EW, Zachariah P, Gorelik M, Boneparth A, Kernie SG, Orange JS, Milner JD. Multisystem inflammatory syndrome related to COVID-19 in previously healthy children and adolescents in New York City. *JAMA* 2020;doi: 10.1001/jama.2020.10374.
7. RCPCH. Paediatric multisystem inflammatory syndrome temporally associated with COVID-19. Available from: https://www.rcpch.ac.uk/resources/guidance-paediatric-multisystem-inflammatory-syndrome-temporally-associated-covid-19.
8. ECDC. Situation update 21 June 2020. Available from: https://www.ecdc.europa.eu/en/covid-19/situation-updates.
9. WHO. Multisystem inflammatory syndrome in children and adolescents with COVID-19. May 15, 2020. Available from: https://www.who.int/publications-detail/multisystem-inflammatory-syndrome-in-children-and-adolescents-with-covid-19.
10. Lopez L, Colan SD, Frommelt PC, Ensing GJ, Kendall K, Younoszai AK, Lai WW, Geva T. Recommendations for quantification methods during the performance of a pediatric echocardiogram: a report from the Pediatric Measurements Writing Group of the American Society of Echocardiography Pediatric and Congenital Heart Disease Council. *J Am Soc Echocardiogr* 2010;**23**:465–495.
11. Pettersen MD, Du W, Skeens ME, Humes RA. Regression equations for calculation of z scores of cardiac structures in a large cohort of healthy infants, children, and adolescents: an echocardiographic study. *J Am Soc Echocardiogr* 2008;**21**: 922–934.
12. Eidem BW, McMahon CJ, Cohen RR, Wu J, Finkelshteyn I, Kovalchin JP, Ayres NA, Bezold LI, O'Brian Smith E, Pignatelli RH. Impact of cardiac growth on Doppler tissue imaging velocities: a study in healthy children. *J Am Soc Echocardiogr* 2004;**17**:212–221.
13. Nagueh SF, Appleton CP, Gillebert TC, Marino PN, Oh JK, Smiseth OA, Waggoner AD, Flachskampf FA, Pellikka PA, Evangelisa A. Recommendations for the evaluation of left ventricular diastolic function by echocardiography. *J Am Soc Echocardiogr* 2009;**22**:107–133.
14. Levy PT, Machefsky A, Sanchez AA, Patel MD, Rogal S, Fowler S, Yaeger L, Hardi A, Holland MR, Hamvas A, Singh GK. Reference ranges of left ventricular strain measures by two-dimensional speckle-tracking echocardiography in children: a systematic review and meta-analysis. *J Am Soc Echocardiogr* 2016;**29**:209–225.
15. Simpson J, Lopez L, Acar P, Friedberg M, Khoo N, Ko H, Marek J, Marx G, McGhie J, Meijboom F, Roberson D, Van den Bosch A, Miller O, Shirali G. Three-dimensional echocardiography in congenital heart disease: an expert consensus document from the European Association of Cardiovascular Imaging and the American Society of Echocardiography. *Eur Heart J Cardiovasc Imaging* 2016; **17**:1071–1097.

16. Dallaire F, Dahdah N. New equations and a critical appraisal of coronary artery Z scores in healthy children. *J Am Soc Echocardiogr* 2011;**24**:60–74.
17. van Stijn-Bringas Dimitriades D, Planken RN, Groenink M, Streekstra GJ, Kuijpers TW, Kuipers IM. Coronary artery assessment in Kawasaki disease with dual-source CT angiography to uncover vascular pathology. *Eur Radiol* 2020;**30**: 432–441.
18. Ferreira VM, Schulz-Menger J, Holmvang G, Kramer CM, Carbone I, Sechtem U, Kindermann I, Gutberlet M, Cooper LT, Liu P, Friedrich MG. Cardiovascular magnetic resonance in nonischemic myocardial inflammation: expert recommendations. *J Am Coll Cardiol* 2018;**72**:3158–3176.
19. Friedman KG, Gauvreau K, Hamaoka-Okamoto A, Tang A, Berry E, Tremoulet AH, Mahavadi VS, Baker A, deFerranti SD, Fulton DR, Burns JC, Newburger JW. Coronary artery aneurysms in kawasaki disease: risk factors for progressive disease and adverse cardiac events in the US population. *J Am Heart Assoc* 2016;**5**: e003289.
20. Joint Working Group JCS. Guidelines for diagnosis and management of cardiovascular sequelae in Kawasaki disease (JCS 2008)—digest version. *Circ J* 2010;**74**: 1989–2020.
21. Scatteia A, Baritussio A, Bucciarelli-Ducci C. Strain imaging using cardiac magnetic resonance. *Heart Fail Rev* 2017;**22**:465–476.
22. Newburger JW, Takahashi M, Beiser AS, Burns JC, Bastian J, Chung KJ, Colan SD, Duffy CE, Fulton DR, Glode MP, Mason WH, Meissner HC, Rowley AH, Shulman ST, Reddy V, Sundel RP, Wiggins JW, Colton T, Melish ME, Rosen FS, A single intravenous infusion of gamma globulin as compared with four infusions in the treatment of acute Kawasaki syndrome. *N Engl J Med* 1991;**324**:1633–1639.
23. Dallaire F, Fournier A, Breton J, Nguyen TD, Spigelblatt L, Dahdah N. Marked variations in serial coronary artery diameter measures in Kawasaki disease: a new indicator of coronary involvement. *J Am Soc Echocardiogr* 2012;**25**:859–865.
24. McCrindle BW, Rowley AH, Newburger JW, Burns JC, Bolger AF, Gewitz M, Baker AL, Jackson MA, Takahashi M, Shah PB, Kobayashi T, Wu MH, Saji TT, Pahl E; American Heart Association Rheumatic Fever, Endocarditis, and Kawasaki Disease Committee of the Council on Cardiovascular Disease in the Young; Council on Cardiovascular and Stroke Nursing; Council on Cardiovascular Surgery and Anesthesia; and Council on Epidemiology and Prevention. Diagnosis, treatment, and long-term management of Kawasaki disease: a scientific statement for health professionals from the American Heart Association. *Circulation* 2017; **135**:e927–e999.
25. Muniz JC, Dummer K, Gauvreau K, Colan SD, Fulton DR, Newburger JW. Coronary artery dimensions in febrile children without Kawasaki disease. *Circ Cardiovasc Imaging* 2013;**6**:239–244.
26. Bratincsak A, Reddy VD, Purohit PJ, Tremoulet AH, Molkara DP, Frazer JR, Dyar D, Bush RA, Sim JY, Sang N, Burns JC, Melish MA. Coronary artery dilation in acute Kawasaki disease and acute illnesses associated with fever. *Pediatr Infec Dis J* 2012;**31**:924–926.
27. Simpson JM, Newburger JW. Multi-system inflammatory syndrome in children in association with COVID-19. *Circulation* 2020;doi: 10.1161/CIRCULATIONAHA. 120.048726.
28. Peng Y, Zeng J, Du Z, Sun G, Guo H. Usefulness of 64-slice MDCT for follow-up of young children with coronary artery aneurysm due to Kawasaki disease: initial experience. *Eur J Radiol* 2009;**69**:500–509.
29. Chu WC, Mok GC, Lam WW, Yam MC, Sung RY. Assessment of coronary artery aneurysms in paediatric patients with Kawasaki disease by multidetector row CT angiography: feasibility and comparison with 2D echocardiography. *Pediatr Radiol* 2006;**36**:1148–1153.
30. Printz BF, Sleeper LA, Newburger JW, Minich LL, Bradley T, Cohen MS, Frank D, Li JS, Margossian R, Shirali G, Takahashi M, Colan SD; Pediatric Heart Network Investigators. Noncoronary cardiac abnormalities are associated with coronary artery dilation and with laboratory inflammatory markers in acute Kawasaki disease. *J Am Coll Cardiol* 2011;**57**:86–92.